Klebsiella aerogenes Urease로의 니켈의 도입

이 만 형 (효성여대)

NICKEL INCORPORATION INTO *Klebsiella aerogenes* UREASE

By

Mann Hyung Lee, Ph. D.

Hyosung Women's University

Abstract

Although ureases play important roles in microbial nitrogen metabolism and in the pathogenesis of several human diseases, little is known of the mechanism of metallocenter biosynthesis in this Ni-containing enzyme.

Klebsiella aerogenes urease apo-protein was purified from cells grown in the absence of Ni. The purified apo-enzyme showed the same native molecular weight, charge, and subunit stoichiometry as the holo-enzyme. Chemical modification studies were consistent with histidinyl ligation of Ni. Apo-enzyme could not be activated by simple addition of Ni ions suggesting a requirement for a cellular factor.

Deletion analysis showed that four accessory genes (*ureD, ureE, ureF,* and *ureG*) are necessary for the functional incorporation of the urease metallocenter. Whereas the Δ*ureD,* Δ*ureF,* and Δ*ureG* mutants are inactive and their ureases lack Ni, the Δ*ureE* mutants retain partial activity and their ureases possess corresponding lower levels of Ni. UreE and UreG peptides were identified by SDS-polyacrylamide gel comparisons of mutant and wild type cells and by N-terminal sequencing. UreD and UreF peptides, which are synthesized at very low levels, were identified by using *in vitro* transcription/translation methods. Cotransformation of *E. coli* cells with the complementing plasmids confirmed that *ureD* and *ureF* gene products act in *trans.*

UreE was purified and characterized. Immunogold electron microscopic studies were used to localize UreE to the cytoplasm. Equilibrium dialysis studies of purified UreE with $^{63}NiCl_2$ showed that it binds ~6 Ni in a specific manner with a K_d of 9.6 ± 1.3 μM. Results from spectroscopic studies demonstrated that Ni ions are ligated by 5 histidinyl residues and a sixth N or O atom, consistent with participation of the polyhistidine tail at the carboxyl termini of the dimeric UreE in Ni binding.

With these results and other known features of the urease-related gene products, a model for urease metallocenter biosynthesis is proposed in which UreE binds Ni and acts as a Ni donor to the urease apo-protein while UreG binds ATP and couples its hydrolysis to the Ni incorporation process.

Introduction

Urease (EC 3. 5. 1. 5) is a nickel-containing enzyme that catalyzes the hydrolysis of urea to form carbonic acid and two molecules of ammonia. Until recently, the best characterized urease was that from jack bean. This enzyme was the first ever to be crystallized (1) and the first shown to possess nickel (2). However, because of the ease of cell growth and genetic manipulation in bacteria compared with plants and because of the medical importance of bacterial urease, our understanding of the prokaryotic enzyme has outpaced knowledge of the plant enzyme (3). In addition to being important in bacterial nitrogen metabolism, bacterial urease has been implicated as an important virulence factor in several human pathogenic states, including those associated with urinary tract infections such as urinary stones, pyelonephritis, ammonia encephalopathy, hyperammonemia, and hepatic coma (For review, see ref. 3). Besides these, potent urease of *Helicobacter pylori* (formerly *Campylobacter pyloridis*) has been implicated in the development of peptic ulcers (4) and type B gastritis (5).

The most extensively characterized microbial urease is that from the gram-negative enteric bacterium *Klebsiella areogenes* (a non-nitrogen-fixing *Klebsiella pneumoniae*). In contrast to the homohexameric jack bean enzyme (subunit M_r = 90,770), the urease of *Klebsiella aerogenes* consists of one large (α; M_r = 60,000 to 75,000) and two distinct small subunits (β and γ; M_r = 8,000 to 11,000). It was shown that the jack bean urease (6) and the *K. aerogenes* enzyme (7) have 2 mol nickel/mol catalytic unit.

DNA sequence analysis of the *Klebsiella aerogenes* urease operon has revealed the presence of several additional genes that are part of the urease gene cluster. The *ureA*, *ureB*, and *ureC* genes encoding the urease subunits are immediately preceded by the *ureD* gene and followed by the *ureE*, *ureF*, and *ureG* genes (8,9).

In this manuscript, it is demonstrated that these accessory genes are involved in some aspect of nickel metallocenter biosynthesis. Purification and characterization of some of these accessory gene products (UreE and UreG) is also described.

Materials and Methods

Plasmid construction. Plasmid DNA was isolated by using the alkaline lysis method of Birnboim (10). Specific DNA fragments generated by restriction endonuclease digestion were isolated by using NA45-DEAE cellulose membranes after electrophoretic separation of DNA fragments on agarose gels. All restriction enzyme digestions, end fillings, and other common DNA manipulations were performed by standard procedures (11). The previously described plasmids pKAU17 (a pUC8 derivative) and pKAU19 (a derivative of pBR328) contain all genes required to express active *K. aerogenes* urease in *Escherichia coli* DH1(12). An *Eco*RI-*Hin*dIII fragment of pKAU17 was isolated by elution from a 1% agarose gel, treated with Klenow fragment of *E. coli* DNA polymerase to produce blunt ends, and inserted into the *Hin*cII site of pUC18 to produce pKAU22 (Fig. 1). The *Nru*I-*Bcl*I, *Bsp*HI-*Rsr*II, and *Aat*II-*Hin*dIII fragments of pKAU17 were cloned separately into the *Eco*RV site (behind the tetracycline promoter) of plasmid pACYC184 (13) to generate plasmids pACYC-D, pACYC-F, and pACYC-G, respectively. In the case of pACYC-D construction, pKAU17 was isolated from *E. coli* GM48 (a *dam* mutant strain), both the *Nru*I-*Bcl*I fragment and the restricted pACYC plasmid were treated with Klenow fragment to generate blunt ends, and the vector was dephosphorylated before ligation.

Deletion mutagenesis. Selective deletions within each of the *ureE*, *ureF*, and *ureG* genes were obtained by using a combination of restriction digestion and *Bal*31 digestion. For the *ureE* deletion, pKAU17 was partially digested with *Stu*I, a *Spe*I linker was inserted into the cleavage sites, the appropriate subclone was identified on the basis of its restriction pattern, the unique *Spe*I site was restricted, the ends were partially digested with *Bal* 31, and the linear fragment was religated after making the ends flush with Klenow fragment. Two clones containing deletions of approximately 190 and 260-bp (designated Δ*ureE-1* and Δ*ureE-2*) were further analyzed as described below. The single *ureF* deletion was generated by removal of the 552-bp *Aat*II-*Avr*II fragment of pKAU17 followed by T4 DNA polymerase treatment to make blunt ends. Two *ureG* mutations containing deletions of approximately 310 and 360-bp (designated Δ*ureG-1* and Δ*ureG-2*) were generated by restriction with *Rsr*II, digestion with *Bal* 31, and religation. Deletion clones were verified by restriction analysis.

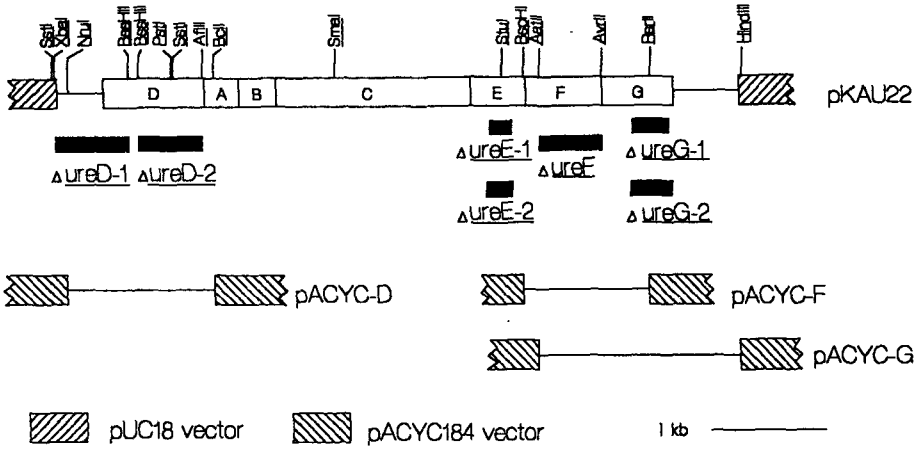

Figure 1. *K. aerogenes* urease gene cluster, selected subclones, and location of deletions in mutanat derivatives. The map of the *K. aerogenes* urease gene cluster in pKAU22 shows the location of the restriction sites used in sequence analysis, isolation of subclones, or generation of deletion derivatives. The sequence to the right of the *Ssfi* site within the *ureD* gene has been published previously (13). Sites of deletions are indicated by solid bars; deletions in *ureD* were generated in pKAU22 whereas deletions in *ureE*, *ureF*, and *ureG* were obtained by using the precursor plasmid, pKAU17, as described in the text. Plasmids pACYC-D, pACYC-F, and pACYC-G are subclones of *ureD*, *ureF*, and *ureG* in the vector pACYC184.

Assays. Urease activity was measured as previously described (12). Protein concentrations were routinely assessed by the spectrophotometric assay of Lowry *et al.* (14) using bovine serum albumin as a standard. Samples were assayed for nickel content using a computer-interfaced Varian SpectraAA-400Z atomic absorption spectrometer after hydrolysis in 1 N HNO_3, drying, and dissolution in 50 mM HNO_3.

Polyacryamide gel electrophoresis. Sodium dodecyl sulfate (SDS)-polyacrylamide gel electrophoresis was carried out by using the buffers of Laemmli (15) and included either a 12 or 15% acrylamide running gel or a 10 to 15% polyacrylamide gradient running gel with a 4.5% polyacrylamide stacking gel. Gels were stained with Coomassie brilliant blue and scanned with a Gilford Response spectrophotometer at 540 nm.

Amino terminal sequencing of accessory proteins. The peptides from partially purified protein fractions were resolved in a 0.75-mm denaturing gel, as described above, and transferred to a sheet of Pro-Blot membrane by standard procedures (16). The bands were visualized by Coomassie blue staining, cut from the membrane, and analyzed by using an Applied Biosystems 477A automated sequencer.

In vitro transcription-translation. Two μg of purified plasmid DNA was transcribed and translated in the presence of [^{35}S]- methionine (1,122 Ci/mmol) in 50 μl of an in vitro transcription-translation reaction mixture according to the manufacturer's instructions (Promega Corp., Madison, Wis.). Aliquots (5 μl) were analyzed by denaturing gel electrophoresis, as described above, with ^{14}C-labeled protein molecular weight markers (Amersham Corp., Arlington Heights, Ill.). Gels were fixed, dried, and used to expose X-ray film overnight.

Purification and characterization of urease from accessory gene mutants. Cell extracts were prepared from *E. coli* DH5 cells containing pKAU17 or plasmids deleted in the individual accessory genes and from control *K. aerogenes* cells containing pKAU19. Cells were disrupted in a French pressure cell and then membranes and cellular debris were sedimented for 90 min at 100,000 x *g*, as previously described (17). In some cases, the cell extracts were applied directly to a Mono-Q (HR 10/10) column equilibrated in 50 mM potassium phosphate – 1 mM EDTA – 1mM β-mercaptoethanol (pH 6.5) and eluted with a multistep gradient of increasing KCl in the same buffer. Alternatively, the cell extracts were subjected to chromatography on columns of DEAE-Sepharose, phenyl-Sepharose, and Mono-Q (HR 5/5). In each

case, urease accounted for greater than 90% of the protein in the final samples.

The purified ureases were compared by denaturing gel electrophoresis as described above. In addition, differences in native relative mass were assessed by gel filtration chromatography by using a Superose 12 (HR 10/30) column equilibrated in 0.2 M KCl – 50 mM phosphate – 1 mM EDTA – 1 mM β-mercaptoethanol (pH 7.0).

Purification of UreE protein. Cultures (3 L) of *K. aerogenes* CG253(pKAU19) or *E. coli* DH5 (pKAU17) were grown to late exponential phase (optical density at 600 nm = 3.5) and harvested by centrifugation. The cells were washed twice with PEB buffer (20 mM potassium phosphate, 0.5 mM EDTA, 1 mM 2-mercaptoethanol [pH 7.2]), resuspended in an equal volume of PEB buffer containing 0.5 mM phenylmethylsulfonyl fluoride, disrupted by three passages through a French pressure cell at 18,000 lb/in^2, and centrifuged at 100,000 x *g* for 90 min at 4^{0}C. The cell extracts were chromatographed on a DEAE-Sepharose column (2.5 by 15 cm) at 4^{0}C, in the same buffer and eluted with a 400 ml-linear salt gradient to 1M KCl. UreE eluted from the column at approximately 0.3 M KCl. The pooled sample was desalted and concentrated by using an Amicon pressure filtration stirred-cell with a YM 10 ultrafiltration membrane in PEB buffer (pH 6.9), applied to a carboxymethyl-Sepharose column (2.5 by 17 cm), and eluted with a linear salt gradient to 0.5 M KCl. Nearly homogeneous UreE that was suitable for most experiments described below eluted approximately at 0.2 M KCl. When necessary, this sample was further purified by using a Mono-S column (0.5 by 5 cm) and a linear gradient to 1 M KCl at room temperature.

Native size and nickel content of UreE protein. The molecular weight for native *K. aerogenes* UreE protein was estimated by using a Superose 12 column (1.0 by 30 cm) in 20 mM potassium phosphate, 0.5 mM EDTA, 1 mM 2-mercaptoethanol (pH 7.4) containing 0.2 M KCl. The column was standardized with thyroglobulin, gamma globulin, ovalbumin, myoglobin, and vitamin B_{12} (M_rs = 670,000, 158,000, 44,000, 17,000, and 1,350; Bio-Rad Laboratories, Richmond, CA). Metal contents of ashed samples were determined by using a Varian Spectra AA-400Z atomic absorption spectrometer.

Equilibrium Dialysis. Equilibrium dialysis of UreE with $^{63}NiCl_2$ (1,455 mCi/mmol) diluted with various concentrations of unlabeled $NiCl_2$ was performed either in a Spectrum 5-cell equilibrium dialyzer or an equilibrium microvolume dialyzer (Hoeffer Scientific Instruments, San Francisco, CA) with precut dialysis membranes (MWCO= 12-14,000). Purified UreE (2 μM) was analyzed for nickel binding in 50 mM sodium phosphate (pH 7.2), 50 mM HEPES (pH 7.2), or 50 mM Tris-HCl (pH 7.6) each containing 0.5 % NaCl to reduce the Donnan effect. After a 3 hr equilibration period at room temperature, radioactivity was measured in aliquots from each compartment by using a Beckman LS7000 liquid scintillation system. Calculation of the bound Ni was performed by standard procedures (18).

Spectroscopic characterization of UreE holoprotein. UreE (35 mg/ml) in the presence of 3.1 mM $NiCl_2$, 0.1 mM EDTA, 20 mM potassium phosphate buffer (pH 7.6), and 30 % glycerol was examined by extended X-ray absorption fine structure (EXAFS) and by variable temperature magnetic circular dichroism (MCD) spectroscopy.

RESULTS AND DISCUSSION

Selective inactivation of *ureD*, *ureE*, *ureF*, and *ureG*. A map of the urease gene cluster indicating deletions within the *ureD*, *ureE*, *ureF*, and *ureG* genes is provided in Fig. 1. Also shown are restriction sites that were used for generating the deletion mutants, for subcloning, and for obtaining fragments for sequence analysis. Extracts of recombinant *E. coli* DH5 cells from a control culture and from each of the deletion mutants were examined for urease activity as shown in Table 1; the Δ*ureE* mutants retain partial activity, whereas the Δ*ureD*, Δ*ureF*, and Δ*ureG* mutants are inactive.

The depressed activity levels in the Δ*ureE* mutants may arise, at least in part, from polar effects on downstream genes which are required for urease activation. As discussed below, SDS-polyacrylamide gel analysis of these cell extracts is consistent with partial polarity. Similarly, the Δ*ureF* mutant could theoretically yield inactive urease because of polar effects on expression of the *ureG* gene; the 552-bp deletion in *ureF* leads to a frame shift at the end of an abbreviated UreF peptide, placing the new termination codon 22 bp

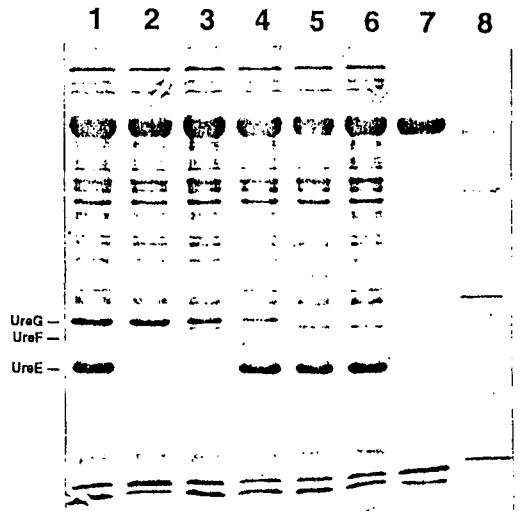

Figure 2. Analysis of deletion mutants by SDS-polyacrylamide gel electrophoresis. Cell extracts from a control *E. coli* DH5 culture containing pKAU17 (lane 1) and from cells containing pKAU17 with deletions in *ureE* (Δ*ureE-1* in lane 2 and Δ*ureE-2* in lane 3), *ureF* (lane 4), or *ureG* (Δ*ureG-1* in lane 5 and Δ*ureG-2* in lane 6) were subjected to SDS-polyacrylamide gel electrophoresis by using a 10-15% gradient gel, followed by Coomassie blue staining. Standard urease (lane 7) and molecular weight markers (lane 8: phosphorylase b, M_r 92,500; bovine serum albumin, M_r 66,200; ovalbumin, M_r 45,000; carbonic anhydrase, M_r 31,000; soybean trypsin inhibitor, M_r 21,500; and lysozyme, M_r 14,400.) were also examined. The proposed locations of the UreE, UreF, and UreG peptides are indicated.

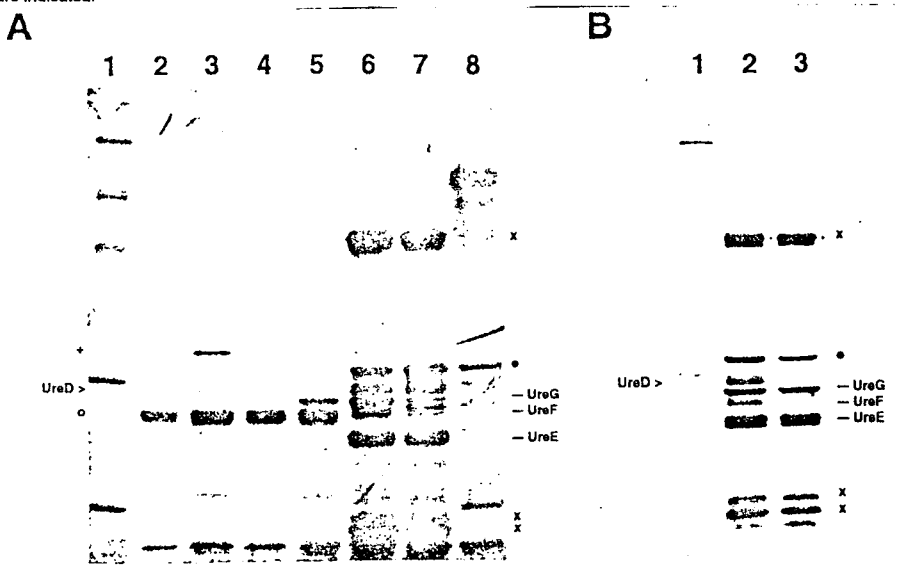

Figure 3. In vitro transcription-translation of urease-related plasmids. Purified DNA was transcribed and translated as described in the Materials and Methods section. After denaturing gel electrophoresis, the peptides obtained in each sample were visualized by exposure to X-ray film. **Panel A**: Radiolabeled molecular weight markers (lane 1) included myosin, M_r 200,000; phosphorylase b, M_r 92,500; bovine serum albumin, M_r 69,000; ovalbumin, M_r 46,000; carbonic anhydrase, M_r 30,000; and lysozyme, M_r 14,300. Lanes 2-5 contain samples from pACYC184 and its derivatives, pACYC-D, pACYC-F, and pACYC-G, respectively. Lane 6 is derived from pKAU17, whereas lane 7 is from pKAU17Δ*ureF*. Lane 8 contains the control plasmid pGEMβGAL, containing the β-lactamase gene. **Panel B**: Molecular weight markers (lane 1), pKAU22 (lane 2), and pKAU22Δ*ureD-1* (lane 3). The positions are shown for UreD, UreE, UreF, and UreG, for the urease subunits (X), for an uncharacterized peptide that is enhanced in pACYC-D (+), and for chloramphenical acetyltransferase (o) and β-lactamase (•).

downstream of the normal position and overlapping the start of *ureG* by 14 bp. To test whether the Δ*ureF* deletion mutant lacks activity because of polarity on *ureG*, cells were cotransformed with the Δ*ureF* plasmid and with a compatible plasmid, pACYC-G, containing an intact *ureG* gene. As shown by the data in Table 1, cotransformation of cells with Δ*ureF* and pACYC-G plasmids does not restore urease activity. In contrast, pACYC-G is capable of restoring activity in cells containing the Δ*ureG* plasmid, demonstrating the ability of the former plasmid to express an active UreG protein. Other cotransformation experiments included the demonstration that an intact *ureD* gene in pACYC-D could restore activity to cells containing Δ*ureD* plasmids, and pACYC-F, containing the *ureF* gene, could restore the Δ*ureF* mutant (Table 1). Thus, *ureD* and *ureF* encode trans-acting factors that are required for generating active urease.

Table 1. Urease specific activities in *E. coli* cell extracts from cells containing control plasmids and derivatives

Plasmid Derivative	Specific Activity[a] (U mg^{-1})
pKAU17	198.4
pKAU17Δ*ureE-1*	105.2
pKAU17Δ*ureE-2*	84.9
pKAU17Δ*ureF*	< 1
pKAU17Δ*ureF* + pACYC-F	66.5
pKAU17Δ*ureF* + pACYC-G	< 1
pKAU17Δ*ureG-1*	< 1
pKAU17Δ*ureG-1* + pACYC-G	129.7
pKAU17Δ*ureG-2*	< 1
pKAU17Δ*ureG-2* + pACYC-G	192.5
pKAU22	141.2
pKAU22Δ*ureD-1*	< 1
pKAU22Δ*ureD-1* + pACYC-D	48.6
pKAU22Δ*ureD-2*	< 1
pKAU22Δ*ureD-2* + pACYC-D	17.2

[a] Cells were grown overnight in LB containing 1 mM nickel chloride, concentrated by centrifugation, sonicated, and assayed for urease activity and protein content.

The extracts from the deletion mutants were subjected to SDS-polyacrylamide gel electrophoresis, as shown in Fig. 2. In each case, the urease subunits were present at high levels and comigrated with purified urease peptides; i.e., the mutations did not affect urease expression. The Δ*ureE* mutants lacked an intense band at an apparent M_r = 23,900 ± 1,000; additionally, in the case of Δ*ureE-2*, bands at M_rs of 27,000 and 28,500 were of diminished intensity. The Δ*ureF* mutant lacked a faint band at an M_r of 27,000 ± 1,000 and exhibited decreased intensity of a band at an M_r of 28,500, but was otherwise unaffected. The Δ*ureG* mutants were only deficient in an intense band at M_r = 28,500 ± 1,000. No changes from the control cultures were observed for Δ*ureD* mutants. These results are consistent with the proposal that the *ureE*, *ureF*, and *ureG* genes encode proteins with M_rs of 23,900, 27,000, and 28,500, respectively, and that the Δ*ureE-2* and Δ*ureF* mutants exhibit partial polarity on downstream genes.

To verify the gene-peptide assignments for the two peptides which were expressed at a high level, their amino-terminal sequences were determined. The putative UreE and UreG peptides possessed sequences (Met-Leu-Tyr-Leu-Thr and Met-Asn-Ser-Tyr-Lys) that were identical to those predicted for these peptides on the basis of their DNA sequences (8). These peptides did not migrate in SDS-polyacrylamide gels according to their sizes (M_rs of 17,558 and 21,943) predicted by DNA sequencing. Gel scanning or visual inspection of Fig. 2 indicates that the UreE and UreG peptides are present at levels that are roughly comparable in intensity to the urease subunits. In contrast, the putative UreF peptide is present at barely detectable levels and UreD was not observed in *E. coli*(pKAU17) or *K. aerogenes*(pKAU19) cell extracts. To enhance the ability to detect plasmid-derived UreD peptide and to provide verification of the UreF peptide assignment, in vitro transcription-translation analysis was performed (Fig. 3). As a control (Fig. 3A, lane 5), the pACYC-G plasmid yielded a unique band at an M_r of 27,000 ± 1,000, consistent with the results described above. The pACYC-D plasmid (Fig. 3A, lane 3) yielded a strong band (M_r = 34,900 ± 1,000) which coincided with a weak band that was also observed in the other pACYC184-derived plasmids (Fig. 3A, lanes 2,4, and 5) and in pKAU17 (Fig. 3A, lane 6). In addition, a faint band (M_r = 29,300 ± 1,000) was observed to be unique to the pACYC-D plasmid (Fig. 3A, lane 3). In a separate experiment comparing the products of pKAU22 and its Δ*ureD-1* derivative (Fig. 3B, lanes 2 and 3), a peptide band (M_r = 29,300 ± 1,000) was clearly missing in the latter sample, identifying this peptide as the *ureD* gene product. No unique band was observed for pACYC-F (Fig. 3A, lane 4), possi-

bly because of overlap with the intense band of plasmid-derived chloramphenicol acetyltransferase at M_r = 25,700 ± 1,000. However, comparison of pKAU17 (Fig. 3A, lane 6) and its Δ*ureF* derivative (Fig. 3A, lane7) clearly shows the loss of a band (M_r = 25,800 ± 1,000) in the latter sample, as observed in cell extracts experiments. Also shown in the two pKAU17 samples are the three urease subunits, the UreE and UreG peptides, and the peptide associated with ampicillin resistance (M_r = 31,800 ± 1,000, also observed in lane 8 containing the pGEMβGAL control plasmid).

Effect of accessory gene mutations on urease. Urease was partially purified from the deletion mutants and from control cells. The specific activities and nickel contents of the mutant proteins are summarized in Table 2. Each of the four genes involved in urease activation affect the level of nickel incorporation into the enzyme.

Table 2. Properties of urease purified from *E. coli* containing intact urease plasmids and deletion mutants

Plasmid derivative	Deleted gene	Specific activity (Umg^{-1})	Number of Ni /catalytic unit
pKAU19	None	2,500	2
pKAU17	None	1,487 (100%)	2.30 (100%)
pKAU22	Δ *ureD-1*	< 1 (0%)	0.15 (7%)
pKAU22	Δ *ureD-2*	< 1 (0%)	0.20 (9%)
pKAU17	Δ *ureE-1*	966 (65%)	1.50 (65%)
pKAU17	Δ *ureE-2*	708 (48%)	1.15 (50%)
pKAU17	Δ *ureF*	< 1 (0%)	< 0.05 (2%)
pKAU17	Δ *ureG-1*	< 1 (0%)	< 0.05 (2%)
pKAU17	Δ *ureG-2*	< 1 (0%)	< 0.05 (2%)

The specific activity of urease purified from *E. coli*(pKAU17) grown in LB containing 1 mM nickel was only 60% of that expected on the basis of the known specific activity of urease purified from *K. aerogenes* (pKAU19) grown in MOPS medium containing 0.1 mM nickel. The low specific activity in the former cells may be related to the very high urease expression levels from this plasmid (urease accounts for well over 20% of the total protein, as illustrated in Fig. 2). Nevertheless, nickel incorporation into urease does not appear to be affected in these samples. The only mutants with significant activity, Δ*ureE-1* and Δ*ureE-2*, had nickel contents that correlated to their specific activities when compared with the pKAU17 control. The reduced nickel contents in urease from these mutants may relate, in part, to partial polar effects on downstream genes. Interestingly, cells containing deletions in *ureE* were more sensitive to growth inhibition at elevated nickel concentrations as if the UreE peptide protected cells from nickel toxicity. Deletions in *ureD*, *ureF*, and *ureG* resulted in the absence of activity and the near absence of nickel. No differences were discerned in the native relative mass of the mutant proteins, as judged by gel filtration chromatography, or in the subunit sizes, as assessed by SDS-polyacrylamide gel electrophoresis.

Purification of UreE. UreE was highly purified by using a combination of DEAE-Sepharose and carboxymethyl-Sepharose column chromatographies. Samples at this stage of purification were estimated to be over 95% homogeneous and were deemed suitable for most of the experiments reported below. In spite of the presence of multiple histidine residues at its carboxyl terminus, UreE did not show any affinity to a chelating-Superose column that was charged with nickel. In contrast, UreE peptide does bind tightly to phenyl-Sepharose resin. Indeed, elution of protein from the hydrophobic resin requires the inclusion of 40% dimethylsulfoxide in the PEB buffer. It is speculated that UreE fails to bind to the resin because the metal ion is transferred from nickel-charged resin to the high affinity nickel-binding site on UreE.

Characterization of UreE: a nickel-binding protein. UreE protein was shown to exist as an apparent dimer (M_r = 35,000) when subjected to gel filtration analysis. When purified in the presence of buffer containing 0.5 mM EDTA, UreE was found to be free of metal ions; however, equilibrium dialysis experiments were used to demonstrate that dimeric UreE binds 6.05 ± 0.05 nickel ions with a K_d of 9.6 ± 1.3 μM (Fig. 4). This value is a combination of the individual values for each of the six nickel sites. Bovine serum albumin (BSA) and lysozyme were used as controls in this experiment. Lysozyme has no reported affinity for nickel ion, whereas, BSA is analogous to the human serum albumin which is known to bind 1 mole of nickel per mole of protein (19).

The specificity of nickel binding was assessed by examining the effects of various concentrations of other divalent cations on

the binding of ^{63}Ni that was present at a concentration of 20 μM (Fig. 5, panel A). The presence of excess magnesium, manganese, and calcium ions had negligible effects on nickel binding even to concentrations of 400 μM. Cobalt ion appeared to compete reasonably well at approximately one of the four sites that bind nickel at this concentration and only weakly competed with the remaining nickel-binding sites. In a separate experiment, 200 μM cobalt was found to have little effect on the total number of nickel that UreE could bind and only slightly shifted the value for K_d (data not shown). Neglecting different affinities for cobalt among the six metal ion sites, the overall apparent K_i for cobalt ion was found to be ~ 640 μM. Copper ion also interferes differentially with the nickel binding sites, but in this case copper ion competed well at approximately three of the four binding sites that bound nickel at 20 μM and competed weakly for the remaining site. Zinc ion exhibited the greatest ability to compete with nickel ion at the concentrations shown, but again this metal preferentially interfered with binding at a subset (approximately half) of the sites. At concentrations higher than 100 μM, zinc ion exhibited anomalous behavior as if it prevented equilibration of nickel ion across the dialysis membrane even in the control sample containing no protein. The presence of distinct nickel-binding sites within UreE is consistent with the cobalt, copper, and zinc competition studies that indicate preferential competition with subsets of the total nickel. The *in vivo* effects of cobalt, copper, and zinc ions on urease metallocenter assembly are unknown; however, Lee *et al.* (20) demonstrated that these cations can not substitute for nickel during urease biosynthesis in the absence of nickel ion.

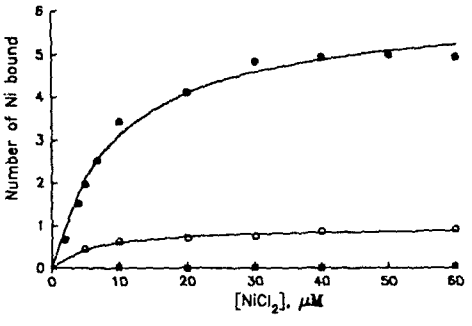

Figure 4. Equilibrium dialysis of UreE with $NiCl_2$. 2 μM UreE (●) in 50 mM sodium phosphate (pH 7.2) buffer containing 0.5% NaCl was equilibrated with the indicated concentrations of $NiCl_2$ solutions containing $^{63}NiCl_2$ (1.2 μCi/ml). Bovine serum albumin (○) and lysozyme (■) were used as controls.

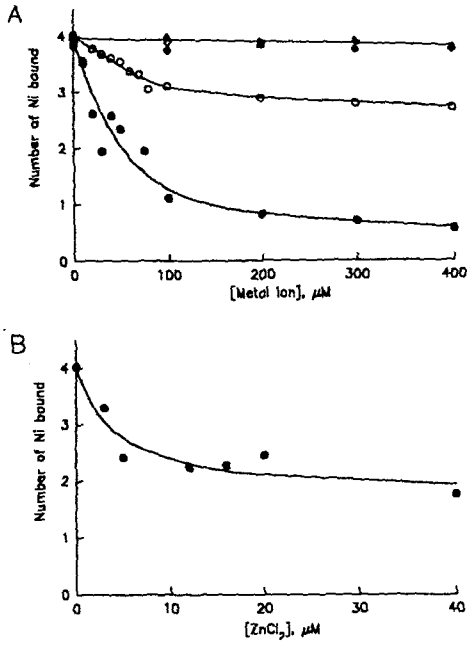

Figure 5. Effect of divalent metal ions on nickel binding to UreE. Equilibrium dialysis of 2 μM of UreE with nickel ion at a concentration of 20 μM was performed in the presence of various concentrations of metal ions. Panel A: Experiments with $MgSO_4$ (◊), $MnCl_2$ (◆), and $CaCl_2$ (▲) were carried out in 50 mM sodium phosphate buffer (pH 7.2), $CoCl_2$ (○) in 50 mM HEPES buffer (pH 7.2), and $CuSO_4$ (●) in 50 mM Tris-HCl buffer (pH 7.6), each containing 0.5 % NaCl. Panel B: Experiments with $ZnCl_2$ were carried out in buffer containing 50 mM sodium phosphate (pH 7.2)-0.5% NaCl. Data at higher concentrations of zinc ion could not be obtained due to anomalous interference with the distribution of Ni ions across the dialysis membrane (See text).

Characterization of the UreE metallocenter. EXAFS data were of high quality and curve fitting required the presence of multiple imidazoles. The best fit to the data assumes a $Ni(imid)_5(N,O)$ coordination sphere. Variable temperature magnetic circular dichroism spectroscopic results were consistent with an octahedral geometry comprised of nitrogen ligands (Fig. 6).

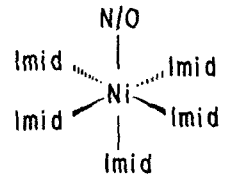

Figure 6. A model of ligand environment Ni bound to UreE based on EXAFS and MCD data.

Conclusions, recent development, and a model. Although the structure and function of metal centers of metalloproteins have received a great deal of attention, very little is known with regard to how these centers are made. Our studies have demonstrated that all four urease accessory genes are necessary for the functional incorporation of the urease metallocenter. It is apparently clear that the accessory proteins do not significantly alter the subunit or native size of the urease protein. Two of the accessory proteins (UreE and UreG) are expressed at levels comparable to those of the urease peptides, whereas UreD and UreF are expressed at undetectable to low levels. It is unclear whether these results reflect stoichiometric or catalytic roles for the proteins.

Although the results with purified UreE clearly demonstrate that the carboxyl terminus of *K. aerogenes* UreE protein can bind nickel ions, it has not been established that this equilibrium process is important for incorporation of nickel into urease. Indeed, the carboxyl termini of UreE peptides from *Proteus mirabilis* (21) and *Helicobacter pylori* (22) possess eight and only one histidine respectively. It is possible, however, that some other protein could functionally compensate for a UreE protein that was deficient in nickel-binding ability. Consistent with this view, deletion of most of the *ureE* gene from a plasmid containing the urease genes does not abolish all urease activity in recombinant *E. coli*, but only reduces the activity levels and correspondingly reduces the nickel content (Table 2). Potential candidates for nickel-binding proteins that could substitute for UreE include auxiliary peptides that are essential for hydrogenase biosynthesis (hydrogenase is another nickel-containing enzyme). For example, ORF5 in the *Azotobacter vinelandii hox* gene cluster possesses a 13-residue region containing 10 histidines (23) and ORF4 in the *Rhodobacter capsulatus hup* gene cluster possesses a region that contains 23 histidines in 62 residues (24). The roles of these hydrogenase-related genes have not been elucidated but they are related in sequence to *hypB*, an *E. coli* gene that is known to function in hydrogenase activation involving nickel incorporation (25).

UreE is only one of the four accessory proteins involved in urease metallocenter assembly. Recently, Park *et al.* (26) have found that UreD copurifies with urease protein when overexpressed by modifying the ribosome-binding site using site-directed mutagenesis and they proposed that UreD may act as a chaperone protein which stabilizes aurease apo-protein conformation that is competent for nickel incorporation. Nothing is known about the functions of *ureF* gene products in this process. Similarly the role of UreG has not been demonstrated; however, sequence analysis reveals a P-loop motif (27) (...**GXXGXGKT**...) that is found in a variety of ATP- and GTP-binding proteins. Furthermore, an energy dependence for *in vivo* nickel ion incorporation was observed (20).

These features, together with the above UreE-related results, lead us to hypothesize that UreE may bind nickel and act as a nickel donor while catalytic UreD holds and stabilizes urease apo-protein rendering its conformation ready for nickel incorporation. UreG hydrolyses ATP and provides energy for the recycling of UreD (Fig. 7). This working model may help to direct future research to understand urease metallocenter assembly process.

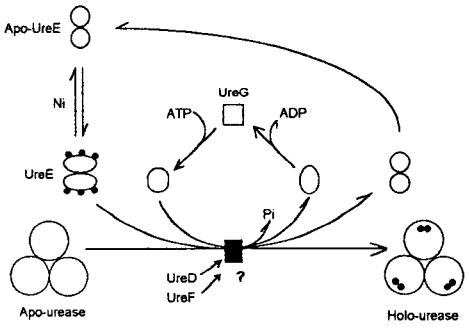

Figure 7. Model of possible roles of accessory gene products in Ni incorporation into *K. aerogenes* urease.

REFERENCES

1. **Sumner, J. B.** 1926. The isolation and crystallization of the enzyme urease. J. Biol. Chem. **69**:435-441.
2. **Dixon, N. E., C. Gazzola, R. L. Blakeley, and B. Zerner**. 1975. Jack bean urease (EC 3.5.1.5). A metalloenzyme. A simple biological role for nickel? J. Am. Chem. Soc. **97**:4131-4233.
3. **Mobley, H. L. T., and R. P. Hausinger.** 1989. Microbial urease: significance, regulation, and molecular characterization. Microbiol. Rev. **53**:85-108.

4. **Hazell, S. L., and A. Lee.** 1986. *Campylobacter pyloridis*, urease, hydrogen ion back diffusion, and gastric ulcers. Lancet. **ii**:15-17.
5. **Graham, D. Y., and P. D. Klein.** 1987. *Campylobacter pyloridis* gastritis: the past, the present, and speculations about the future. Am. J. Gastroent. **82**:283-286.
6. **Dixon, N. E., C. Gazzola, R. L. Blakeley, and B. Zerner.** 1975. Inhibition of jack bean urease (EC 3.5.1.5) by acetohydroxamic acid and by phosphoramidate. An equivalent weight for urease. J. Am. Chem. Soc. **97**:4130-4131.
7. **Todd, M. J., and R. P. Hausinger.** 1989. Competitive inhibitors of *Klebsiella aerogenes* urease: mechanisms of interaction with the nickel active site. J. Biol. Chem. **264**:15835-15842.
8. **Mulrooney, S. B., and R. P. Hausinger.** 1990. Sequence of the *Klebsiella aerogenes* urease genes and evidence for accessory proteins facilitating nickel incorporation. J. Bacteriol. **172**:5837-5843.
9. **Lee, M. H., S. B. Mulrooney, M. J. Renner, Y. Markowicz, and R. P. Hausinger.** 1992. *Klebsiella aerogenes* urease gene cluster: sequence of *ureD* and demonstration that four accessory genes (*ureD, ureE, ureF*, and *ureG*) are involved in nickel metallocenter biosynthesis. J. Bacteriol. **174**:4324-4330.
10. **Birnboim, H. C.** 1983. A rapid alkaline extraction method for the isolation of plasmid DNA. Meth. Enzymol. **100**:243-255.
11. **Sambrook, J., E. F. Fritsch and T. Maniatis.** 1989. Molecular cloning: a laboratory manual. Cold Spring Harbor Laboratory, Cold Spring Harbor, N.Y.
12. **Mulrooney, S. B., H. S. Pankratz and R. P. Hausinger.** 1989. Regulation of gene expression and cellular localization of cloned *Klebsiella aerogenes* (*K. pneumoniae*) urease. J. Gen. Microbiol. **135**:1769-1776.
13. **Chang, A. C. Y, and S. N. Cohen.** 1978. Construction and characterization of amplifiable multicopy DNA cloning vehicles derived from the P15A cryptic miniplasmid. J. Bacteriol. **134**:1141-1156.
14. **Laemmli, U. K.** 1970. Cleavage of structural proteins during assembly of the head of bacteriophage T4. Nature (London) **227**:680-685.
15. **Lowry, O. H., N. J. Rosebrough, A. J. Farr, and R. J. Randall.** 1951. Protein measurement with the folin pheno reagent. J. Biol. Chem. **193**:265-275.
16. **Matsudaira, P.** 1990. Limited N-terminal sequence analysis. Methods Enzymol. **182**:602-613.
17. **Todd, M. J., and R. P. Hausinger.** 1987. Purification and characterization of the nickel-containing multicomponent urease from *Klebsiella aerogenes*. J. Biol. Chem. **262**:5963-5967.
18. **Bell, J. E., and E. T. Bell.** 1988. *In* Proteins and enzymes. pp. 378-399. Prentice-Hall, Inc., Englewood Cliffs, NJ.
19. **Glennon J. D., and B. Sarkar.** 1982. Nickel(II) transport in human blood serum. Biochem. J. **203**:15-23.
20. **Lee, M. H., S. B. Mulrooney, and R. P. Hausinger.** 1990. Purification, characterization, and in vivo reconstitution of *Klebsiella aerogenes* urease apoenzyme. J. Bacteriol. **171**:4427-4431.
21. **Jones, B. D., and H. L. T. Mobley.** 1989. *Proteus mirabilis* urease: nucleotide sequence determination and comparison with jack bean urease. J. Bacteriol. **171**:6414-6422.
22. **Cussac, V., R. I. Ferrero, and A. Labigne.** 1992. Expression of *Helicobacter pylori* urease genes in *Escherichia coli* grown under nitrogen-limiting conditions. J. Bacteriol. **174**:2466-2473.
23. **Chen, J. C., and L. E. Mortenson.** 1992. Identification of six open reading frames from a region of the *Azotobacter vinelandii* genome likely involved in dihydrogen metabolism. Biochim. Biophys. Acta **1131**:199-202.
24. **Xu, H.- W., and J. D. Wall.** 1991. Clustering of genes necessary for hydrogenase oxidation in *Rhodobacter capsulatus*. J. Bacteriol. **173**:2401-2405.
25. **Lutz, S., A. Jacobi, V. Schlensog, R. Böhm, G. Sawers, and A. Böck.** 1991. Molecular characterization of an operon (*hyp*) necessary for activity of the three hydrogenase isozymes in *Escherichia coli*. Mol. Microbiol. **5**:123-135.
26. **Park, I.- S., M. B. Carr, and R. P. Hausinger.** 1994. *In vitro* activaiton of urease apoprotein and role of UreD as a chaperone required for nickel metallocenter assembly. Proc. Natl. Acad. Sci. **91**:3233-3237.
27. **Saraste, M., P. T. Sibbald, and A. wittinghofer.** 1990. The P-loop: a common motif in ATP- and GTP-binding proteins. Trends Biochem. Sci. **15**:430-434.